VIZUALIZATION OF WAVEFRONT DISLOCATIONS OF OPTICAL SPECKLE-FIELDS

V.P. Aksenov, V.A. Banakh, and O.V. Tikhomirova

Institute of Atmospheric Optics,
Siberian Branch of the Russian Academy of Sciences, Tomsk
Received August 26, 1997

Feasibility of noninterferometric techniques of the phase distribution measurements in the laser beam cross-section for visualization of the vortex dislocations of optical speckle-field wave fronts are analyzed. It has been established that the diffraction Hartmann sensor and wave front sensor based on measurements of the intensity in the beam cross-section allow the positions of the dislocation centers to be obtained and spatial configuration of the intensity zero-lines to be retrieved.

Light propagation through a randomly inhomogeneous medium leads to random distortions of the amplitude and phase of optical field due to interference, and the spatial distribution of intensity has a speckle structure. Study of speckle fields may help solve problems of adaptive optics, star speckle-interferometry, and image reconstruction. It is a remarkable peculiarity of the speckle fields that there are dislocations in such fields which are the areas where the optical wave phase becomes undetermined and the intensity vanishes. The dislocations may exist in free space and completely determine the field structure. The wave front in the vicinity of a dislocation point is a helicoid with the axis along the amplitude zero line (Fig. 1).

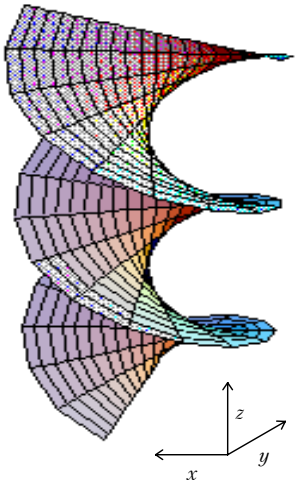

FIG. 1. Wave front in the vicinity of a dislocation.

The most widely spread way of experimentally studying the dislocations is interferometric or holographic[2,3] recording of optical speckle fields. Defects in the wave front develop on interferograms as "forks" or branching of the interference fringes. The bifurcation points coincide with the intensity zeros which can not be distinguished from nonzero local minima of the intensity against the background of a random speckle structure. Moreover, the occurrence isolated intensity zero is not a sufficient condition for the screw dislocation existence at a given point. As an example, it is worth considering the intensity of a wave field which is a difference between the fields of two coaxial Gaussian beams.

Interference methods of wave field diagnostics[2,3] are sufficiently difficult to perform and not always applicable for practical measurements. Therefore, it is useful to consider the methods of identifying the wave front dislocations on the basis of the measurements of intensity distribution $I(\boldsymbol{\rho}, z)$ in the beam cross-section $\boldsymbol{\rho}\{x, y\}$ and to compare their potentialities with those of the diffraction wave front sensors, for example, Hartmann sensors.[4]

The field of a Gauss–Laguerre optical beam was chosen as a test object since the phase front of such a field has all features characteristic of the wave fronts in optical speckle fields. It is known,[5] that slowly varying amplitude of a Gauss–Laguerre optical field generated with a resonator composed of spherical mirrors is written as follows:

$$U(r, \varphi) = \sum_{m,n} g_{mn\pm} A_{mn\pm}(r, \varphi); \qquad (1)$$

$$A_{mn\pm}(r, \varphi) = \sqrt{\frac{4r^2\, m!}{\pi\,(m+1)!}}\, L_m^n(2r^2) \exp\{-r^2 \pm in\varphi\},$$

where m and n are the radial and angular mode indices; $r = \sqrt{x'^2 + y'^2}$ and $\varphi = \arctan(y'/x')$ are the polar coordinates, x' and y' are the Cartesian coordinates normalized by the effective beam radius a; $g_{mn\pm}$ are the complex mode amplitudes; L_m^n is the Laguerre

0235-6880/97/12 998-03 $02.00

polynomial. It is an important property of the Gauss–Laguerre modes,[5,6] when they degenerate, that in this case the laser emission frequency is determined by a combination of the transverse mode indices $l = 2m + n$. For example, when $l = 1$ the degenerate family consists of two modes[5] and in the steady state the initial field has one dislocation on the beam axis. When $l = 2$ the degenerate family consists of three modes[5]

$$A_{10} = \sqrt{2/\pi}\,(1 - 2r^2)\exp\{-r^2\};$$
$$A_{021} = \sqrt{2/\pi}\,2r^2\exp\{-r^2 + 2i\varphi\};$$
$$A_{022} = \sqrt{2/\pi}\,2r^2\exp\{-r^2 - 2i\varphi\};$$
$$U(r,\varphi,0) = A_{10}(r,\varphi)g_1 + A_{021}(r,\varphi)g_2 + A_{022}(r,\varphi)g_3. \quad (2)$$

At a distance z from the source the field, after substitution of Eq. (17) into the Kirchhoff integral, takes the form

$$U(x, y, z) = \Omega\,(1 + \Omega^2)^{-3/2}\exp\{3i\arctan\Omega + \frac{\Omega}{2}\frac{x^2 + y^2}{(1 + \Omega^2)}(i - \Omega)\}\,g, \quad (3)$$

where $\Omega = ka^2/z$ is the diffraction parameter, k is the wave number. The number of dislocations in the beam cross-section depends on[5] ratios between the amplitudes g_1, g_2, and g_3. The intensity and phase distributions in the plane $\Omega = 1$ in the case of four wave front dislocations ($g_1 = 1 + i$, $g_2 = -g_3 = g_1/\sqrt{2}$), are shown in Fig. 2.

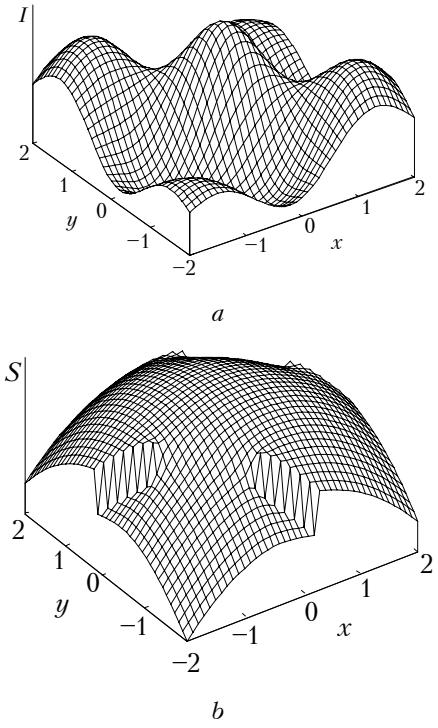

FIG. 2. Phase distribution (a) and intensity distribution (b) in the beam cross-section.

The phase dislocation distortions restrict the efficiency of correction or inversion of wave front with the use of deformable mirrors, since the mirror surface can not be transformed into the surface with the screw dislocation without violation of the continuity condition. Therefore a problem arises on obtaining a smoothed approximation of a wave front. In Ref. 7 we proposed to use the potential phase as such an approximation

$$S_p(\rho, z) = \frac{k}{4\pi^2}\iint\limits_D \frac{d^2\rho_0}{I(\rho_0, z)}\frac{\partial}{\partial z}\times$$
$$\times\int\limits_{-\infty}^{\infty}\int d^2\rho_0'\,\frac{I(\rho_0', z)(\rho_0 - \rho_0')(\rho - \rho_0)}{(\rho_0 - \rho_0')^2(\rho - \rho_0)^2}, \quad (4)$$

reconstructed in the area of the entrance pupil D bounded by the contour Γ from the potential component of the Umov–Pointing vector $\boldsymbol{\mathcal{L}}_p(\rho, z) = I(\rho, z)\nabla S_p(\rho, z)$. The whole Umov-Pointing vector consists of the potential and vortex components

$$\mathcal{L}(\rho, z) = I(\rho, z)\nabla S(\rho, z) = \mathcal{L}_p(\rho, z) + \mathcal{L}_v(\rho, z). \quad (5)$$

In the diffraction sensors the wave front slopes $\mu(x, y) = \frac{\partial}{\partial x}S(x, y)$ and $\nu(x, y) = \frac{\partial}{\partial y}S(x, y)$ are measured and then the phase is retrieved, as a rule, based on solution of the system of linear equations. In this case, as was pointed in Refs. 8 and 9, a task to find the phase becomes equivalent to solving of the Poisson equation

$$\Delta_\perp S(x, y) = \frac{\partial}{\partial x}\mu(x, y) + \frac{\partial}{\partial y}\nu(x, y) \quad (6)$$

with the boundary condition Γ: $S(x, y)|_\Gamma = 0$. It is obvious that when the vector field of the phase gradient $\nabla_\perp S(x, y)$ has a solenoidal component $\nabla_\perp S_s(x, y)$ for which $\nabla_\perp\cdot\{\nabla_\perp S_s(x, y)\} = 0$ (for the divergent component the condition $\nabla_\perp \times \{\nabla_\perp S_\partial(x, y)\} = 0$) then, when solving Eq. (6), we obtain the filtered value of the phase, i.e., its divergent component $S_\partial(x, y)$ corresponding to the divergent component of the whole phase gradient

$$\nabla_\perp S(x, y) = \nabla_\perp S_\partial(x, y) + \nabla_\perp S_s(x, y). \quad (7)$$

It is just the solenoidal component that makes the main peculiarity of the structure of wave fronts with dislocations. Moreover, this component increases, with increasing turbulence intensity along the path or increasing length of the path. Therefore, conventional procedures of the phase correction based on compensation for $\nabla_\perp S_\partial(x, y)$ give poor results under conditions of strong intensity fluctuations.[9]

The divergent phase $S_\partial(x, y)$ is calculated by the Poisson integral formula[10] for the case when D is the circle of radius R

$$S_\partial(\rho, z) = \iint_D \left[\frac{\partial}{\partial x}\mu(\mathbf{r}, z) + \frac{\partial}{\partial y}\nu(\mathbf{r}, z)\right] G(\mathbf{r}, \rho)\, d\mathbf{r}; \quad (8)$$

$$G(\mathbf{r}, \rho) = \frac{1}{4\pi} \ln \frac{R^2 + r^2\rho^2/R^2 - 2r\rho\,\Gamma os(\varphi - \varphi')}{r^2 + \rho^2 - 2r\rho\,\Gamma os(\varphi - \varphi')};$$

$\mathbf{r}\ \{r\cos\varphi', r\sin\varphi'\}$, $\boldsymbol{\rho}\ \{\rho\cos\varphi, \rho\sin\varphi\}$.

Figure 3*a* presents the beam potential phase, retrieved by formula (4) for four dislocations and Fig. 3*b* presents the divergent phase calculated using Eq. (8). In both cases the phase distributions obtained allow the wave front dislocations to be identified and localized. But the potential phase is retrieved from the measurements of intensity distributions in two beam cross-sections and the measurements of local slopes of wave front by Hartmann matrix is the much more complicated problem.[4]

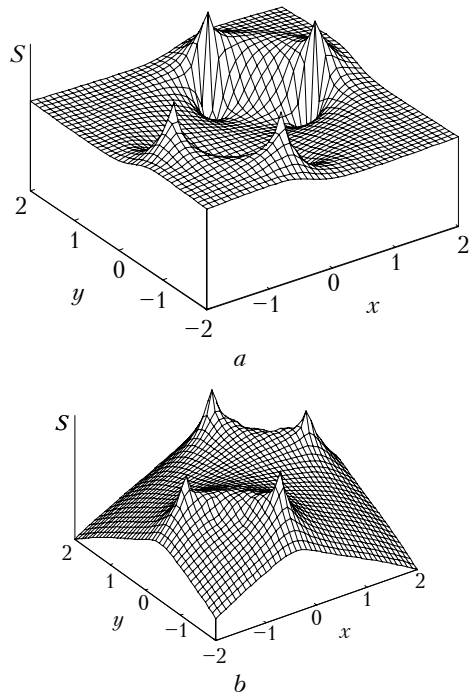

FIG. 3. Potential phase (a) and divergent phase (b).

Let us now consider a question on the relation between the potential and vortex phases introduced in our previous paper[7] and determined by the potential and vortex components of the Umov–Pointing vector with the divergent and solenoidal phases. It is evident, that every term of the whole Umov–Pointing vector

$$\mathcal{L}_\perp(x, y) = I(x, y)\,\nabla_\perp S(x, y) = I(x, y)\,\nabla_\perp S_\partial(x, y) + I(x, y)\,\nabla_\perp S_s(x, y), \quad (9)$$

can be presented as a sum of the potential and vortex components in the general case. Therefore, $\mathcal{L}_{\perp p}$ and, consequently, $\nabla_\perp S_p(x, y)$, have components, depending on the divergent and solenoidal components of the phase gradient. The vortex component of the Umov–Pointing vector and vortex phase are formed in the same manner, therefore, the potential and divergent phases do not coincide in the general case. They are equal to each other when the field has a single dislocation and $\nabla_\perp I(x, y) \times \nabla_\perp S_\partial(x, y) = 0$ and $\nabla_\perp I(x, y) \cdot \nabla_\perp S_s(x, y) = 0$.

Preliminary calculation of the wave aberration[4] shows that the use of the potential phase to make corrections for phase distortions in the adaptive optical system working in the turbulent atmosphere is not more effective than the use of the divergent phase. The explanation is that the potential phase contains not all the divergent phase although it includes a part of the solenoidal one.

Thus, measurements of the potential and divergent phases allow us to localize the centers of the screw dislocations of the optical beam wave front and, therefore, to find positions of the exact intensity zeros which are the indicators of dislocations and can not be selected against the background of numerous local minima in the random transverse distribution of the speckle field intensity. Combination of such zero points corresponding to different values of the longitudinal coordinate z allows the positions of zero lines which are the "skeletonB of the wave field[11] to be reconstructed.

ACKNOWLEDGMENT

This research was supported by "The Open Society InstituteB (Grant A97–1312).

REFERENCES

1. M. Berry, *Singularities in Waves and Rays. Les Houches Summer School* (North-Holland, Amsterdam, 1980), pp. 453–543.
2. B.D. Bobrov, Kvant. Elektron. **18,** No. 7, 886–890 (1991).
3. M.S. Soskin, M.V. Vasnetsov, I.V. Basistiy, Proc. SPIE **2647,** 57–62 (1995).
4. M.A. Vorontsov, A.V. Koryabin, and V.I. Shmal'gauzen, *Controlled Optical System* (Nauka, Moscow, 1988), 272 pp.
5. M. Brambilla, F. Battipede, L.A. Lugiato, V. Penna, F. Prati, C. Tamm, and C.O. Weiss, Phys. Rev. **A43,** No. 9, 5090–5113 (1991).
6. Yu.A. Anan'ev, *Optical Resonators and Problem of Laser Radiation Divergence* (Nauka, Moscow, 1979), 328 pp.
7. V.P. Aksenov, V.A. Banakh, and O.V. Tikhomirova, Atmos. Oceanic Opt. **9,** No. 11, 921–925 (1996).
8. A.N. Bogaturov, Izv. Vyssh. Uchebn. Zaved. SSSR, Ser. Fizika **28,** No. 11, 86–95 (1985).
9. V.P. Lukin and B.V. Fortes, Atmos. Oceanic Opt. **8,** No. 3, 223–230 (1995).
10. G.A. Korn and T.M. Korn, *Mathematical Handbook for Scientists and Engineers* (McGraw-Hill, New York, 1961).
11. V.A. Zhuravlev, I.K. Kobozev, and Yu.A. Kravtsov, Zh. Eksp. Teor. Fiz. **102,** No. 2 (8),483–494 (1992).